*European Cells and Materials* Vol.54 2025 (pages 79–90) DOI: 10.22203/eCM.v054a06 ISSN 1473-2262

*Original Article*

# COMPARATIVE EVALUATION OF RESORBABLE AND NON-RESORBABLE REINFORCED SPACE-MAINTAINING MEMBRANES FOR GUIDED BONE REGENERATION

E.A. Todd[1], V.V. Nayak[2,3,*], K.K. Tadisina[4], E.A. Bonfante[5], Z.J. Liu[6], O. Velazquez[2,6,7], S. Daunert[2,3], N. Tovar[8], L. Witek[9,10,11,12] and P.G. Coelho[2,3,4,13]

[1]University of Miami Miller School of Medicine, Miami, FL 33136, USA
[2]Department of Biochemistry and Molecular Biology, University of Miami Miller School of Medicine, Miami, FL 33136, USA
[3]Dr. John T. Macdonald Foundation Biomedical Nanotechnology Institute (BioNIUM), University of Miami, Miami, FL 33136, USA
[4] DeWitt Daughtry Family Department of Surgery, Division of Plastic Surgery, University of Miami Miller School of Medicine, Miami, FL 33136, USA
[5]Department of Prosthodontics and Periodontology, University of São Paulo-Bauru School of Dentistry, 17012-901 Bauru, São Paulo, Brazil
[6]Department of Surgery, University of Miami Miller School of Medicine, Miami, FL 33136, USA
[7]Department of Interventional Radiology, UMHC-SCC, Miami, FL 33136, USA
[8]Private Practice, Boynton Beach, FL 33436, USA
[9]Biomaterials and Regenerative Biology Division, NYU College of Dentistry, New York, NY 10010, USA
[10]Department of Biomedical Engineering, NYU Tandon School of Engineering, Brooklyn, NY 11201, USA
[11]Hansjörg Wyss Department of Plastic Surgery, NYU Grossman School of Medicine, New York, NY 10016, USA
[12]Department of Oral and Maxillofacial Surgery, NYU College of Dentistry, New York, NY 10010, USA
[13]Sylvester Comprehensive Cancer Center, University of Miami Miller School of Medicine, Miami, FL 33136, USA

**Abstract**

**Background:** Alveolar ridge preservation following tooth extraction remains a clinical challenge, necessitating guided bone regeneration (GBR). The aim of this study was to compare the biocompatibility and tissue response of an experimental resorbable collagen (rCOL) membrane reinforced by poly-lactic-co-glycolic acid to a commercially available non-resorbable titanium (Ti)-reinforced polytetrafluorethylene (rPTFE) membrane in a large translational (beagle) mandibular model. **Materials and Methods:** Beagles (N = 7) underwent bilateral extraction of mandibular premolars, with full-thickness flaps raised to expose the mandibular bone. Bilateral four-walled semi-saddle defects (2 defects per animal) were created using a low-speed cylindrical burr under copious irrigation. Defects were filled with porcine xenograft (Xe) putty and covered with either an experimental rCOL, or commercially-available rPTFE (Cytoplast® Ti-150, Osteogenics Biomedical, Inc., Lubbock, TX, USA) membrane. Animals were allowed to heal for 6 weeks and defects were evaluated by microcomputed tomography ($\mu$CT) and histological analysis. **Results:** $\mu$CT demonstrated gradual bone ingrowth and bone graft bridging within the defects in both membrane groups. However, bone formation within the defects was significantly greater in defects treated with rCOL (27.15 $\pm$ 6.22 %) relative to rPTFE (17.84 $\pm$ 6.22 %) ($p$ = 0.041). Histological evaluation demonstrated that the rPTFE group presented with inflammatory infiltrate and granulation tissue between the defect and membrane surface. In contrast, the defects covered by the rCOL membrane evidenced direct contact with newly formed osseous and connective tissue layers. **Conclusions:** rCOL membranes demonstrated superior healing outcomes characterized by minimal inflammation and higher levels of bone ingrowth within the defect site, compared to rPTFE counterparts.

**Keywords:** Guided bone regeneration, resorbable membranes, alveolar ridge, non-resorbable membranes.

***Address for correspondence**: V.V. Nayak, Department of Biochemistry and Molecular Biology, University of Miami Miller School of Medicine, Miami, FL 33136, USA; Dr. John T. Macdonald Foundation Biomedical Nanotechnology Institute (BioNIUM), University of Miami, Miami, FL 33136, USA. Email: vxn188@miami.edu.

## Introduction

The catabolic alterations following tooth loss commences with the resorption of the bundle bone, a tooth-dependent structure that delineates the extraction socket, necessitating alveolar ridge preservation and/or augmentation via guided bone regeneration (GBR) [1,2]. GBR is an evidence-based, clinically validated, and safe method for extraction site management [3]. In particular clinical scenarios such as cases with thin bone plates (<1 mm) or reduced ridge heights following extraction, GBR enables successful implant placement by reducing the extent of soft and hard tissue dimensional loss [3]. Comparative radiographic assessments indicate that GBR is more effective in preserving bone dimensions relative to socket seal technique or unassisted socket healing [4]. GBR entails the use of occlusive membranes to segment bone volume by excluding non-osteogenic cell populations from the underlying compartmentalized bony defect site. When isolating the non-osteogenic cells, the osteogenic cell populations from the native bone walls are allowed to inhabit the osseous wound, facilitating favorable conditions for adequate new bone formation [5]. GBR membranes hence function as mechanical barriers and play a crucial role during the healing of the alveolar ridge [5]. In addition to preventing epithelial and connective tissue migration into the defect area, GBR membranes are critical in the maintenance of sufficient space within the defect site during the application of masticatory/physiological forces [6]. An ideal GBR membrane must therefore present biocompatibility, clinical manageability, space-making ability, and adequate mechanical stability [7].

The compositions of a GBR membrane can be divided into resorbable and non-resorbable types. Non-resorbable membranes include synthetic fluoropolymers such as polytetrafluoroethylene (PTFE) [7,8]. GBR membranes composed of high density-polytetrafluoroethylene (d-PTFE) have been widely utilized for vertical bone augmentation procedures owing to robust mechanical and occlusive properties [6,9]. A subset of PTFE membranes reinforced with titanium (Ti) was previously developed to serve a mechanical barrier capable of preventing soft tissue migration, protecting the blood clot to achieve vertical hard tissue gain, and providing mechanical stability at the tented defect site [10]. However, an unfavorable outcome with the use of non-resorbable membranes is wound dehiscence [11,12]. For example, wound dehiscence has been shown to result in susceptibility to the exposure field with progression of the infection, inadequate bone healing, and graft material loss [6]. Another disadvantage of non-resorbable membranes is the need for a secondary surgery for membrane removal [11].

On the other hand, resorbable collagen membranes have been extensively utilized in GBR procedures, with a long-standing database of evidence in tissue regeneration owing to low immunogenicity, cell adhesive properties, and chemotaxis to fibroblasts and osteoblasts, thereby mediating excellent tissue integration and angiogenesis [6,7,13]. However, poor mechanical properties and high degradation rates of native collagen-based barrier membranes are still dominant limitations during clinical applications [9]. In the maxillofacial region where significant host tissue movement occurs during the healing period, mechanical stability is essential for predictable recovery [14]. To elaborate, the success of GBR is also related to the mechanical properties of the membrane, which can influence whether the membrane collapses into the defect space, or if the amount of regenerated bone in the bone defect is reduced [7]. To prevent undesirable outcomes, GBR membranes should be sufficiently rigid to withstand the compression of the overlying soft tissue [7]. Additionally, it should present a degree of plasticity which would enable easy contouring and shaping/draping over the defect [7].

Mechanical reinforcement is one such strategy to modify the mechanical characteristics of collagen-based devices. By reinforcing with a second biomaterial, the strength or handling characteristics of the membrane can be modified while maintaining the biological benefits of collagen. Poly-lactic-co-glycolic acid (PLGA) belongs to a class of synthetic, biodegradable, biocompatible copolymers that has been utilized in the fabrication of resorbable sutures, surgical clips, and implantable/injectable controlled-release drug delivery systems [15]. *In vivo*, PLGA induces minimal inflammatory responses and resorbs over time through the hydrolysis of ester linkages into lactic and glycolic acids [15]. The adjustable lactic: glycolic acid ratio in PLGA further allows tunable degradation rates (2–6 months) which synchronizes with the critical 3-month bone healing window [16]. This contrasts with rapidly-resorbing collagen-based materials (<8 weeks) that could compromise barrier function prematurely. Building on these findings, a PLGA mesh-reinforced resorbable collagen (rCOL)-based membrane was recently introduced [14]. However, from a data availability and consensus standpoint, there is lacking literature that directly compares this reinforced resorbable membrane to a more widely-utilized reinforced non-resorbable polytetrafluorethylene (rPTFE) membrane in a large translational model to ensure their efficacy and reliability for potential clinical use. This study specifically aimed to evaluate the biocompatibility and tissue response of rCOL and rPTFE membranes via histomorphometric and micro-computed tomographic analyses in a beagle mandibular model.

## Materials and Methods

### *Materials*

The commercially available non-resorbable membrane (rPTFE: Batch No.: A057070; Cytoplast® Ti-150, 25 mm × 30 mm, Osteogenics Biomedical, Inc., Lubbock, TX, USA) presented a textured (Regentex™) d-PTFE outer layer to increase the surface area available

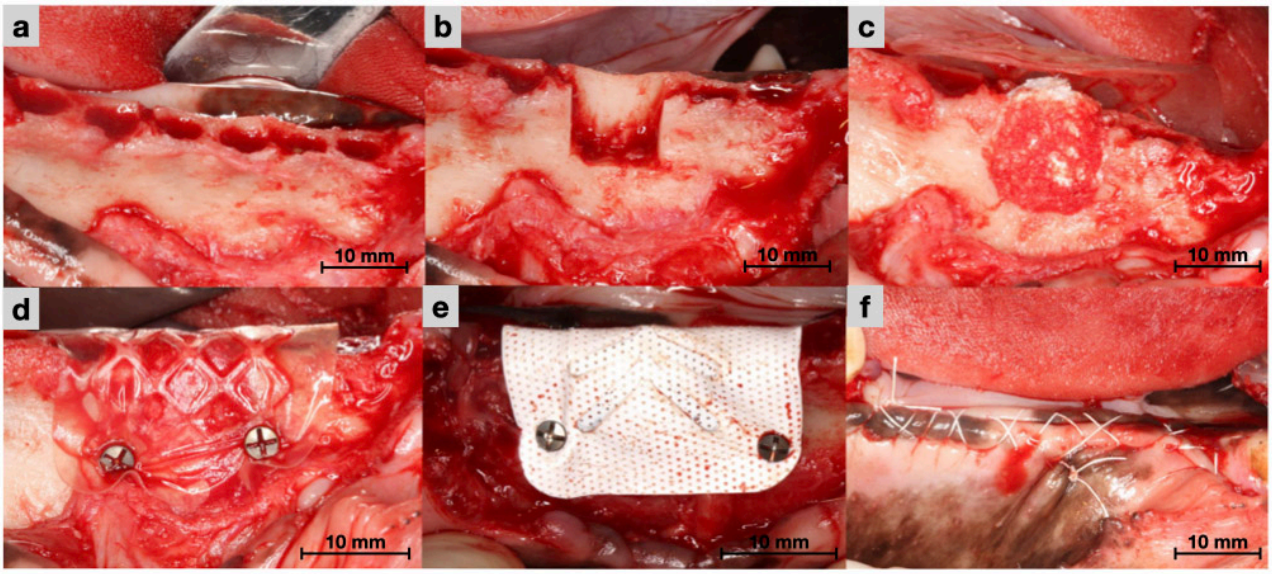


**Fig. 1. Surgical aspect of the mandible.** Surgical aspect from the buccal view (**a**) post-teeth extraction, (**b**) after the creation of the four-walled semi-saddled defect, (**c**) showing the defect filled with porcine xenograft putty, (**d**) with a resorbable membrane (rCOL) overlaying the defect on the anatomic right side, (**e**) with a non-resorbable (rPTFE) membrane overlaying the defect on the anatomic left side, (**f**) showing defects sutured close. Scale bars are 10 mm in length. rCOL, reinforced collagen; rPTFE, reinforced polytetrafluorethylene.

for cellular attachment and to prevent soft tissue retraction. This was accompanied by an intermediate grade 1 titanium framework, and an expanded PTFE (e-PTFE) inner layer [10]. On the other hand, the patented, experimental, resorbable membrane (rCOL, Batch No.: RD001-1; 20 mm × 30 mm, Osteogenics Biomedical, Inc., Lubbock, TX, USA) comprised of decellularized, natural (porcine pericardium-derived) collagen-based inner- and outer- surfaces and a bioresorbable PLGA mesh embedded between the two collagen layers [14]. It is also important to note that the inner- and outer- decellularized natural collagen-based membranes were cross-linked to each other followed by caprylic odor removal, lyophilization, and die cutting, as previously described [14].

*Preclinical In Vivo Model*

According to a sample size calculation for statistical power greater than 0.8, an effect size of 0.65, and type I error frequency ($\alpha$) of 0.05, a total of N = 7 adult, skeletally mature, female beagle dogs aged ~ 1.5 years and in good health (10–15 kg) were utilized. The animals were allowed to acclimate at École Nationale Vétérinaire d'Alfort (ENVA) for 7 days prior to the surgery. On the day of surgery, subjects were fasted for at least 12 hours to prevent vomiting due to anesthesia. All surgical procedures were conducted under general anesthesia using veterinary pharmaceutical-grade agents. The pre-anesthetic procedure comprised of an intramuscular administration of atropine sulfate (strength: 0.54 mg/mL, administered at: 0.044 mg/kg, Batch No.: 51662-1311; Sparhawk Laboratories Inc., Lenexa, KS, USA, NDC 58005-354-04) and xylazine hydrochloride (strength: 20 mg/mL, administered at: 8 mg/kg, Batch No.: NC-0528; CP-Pharma Handelsgesellschaft mbH, Burgdorf, Germany, AMM FR/V/4410949 3/2012). General anesthesia was provided using an intramuscular injection of ketamine hydrochloride (strength: 100 mg/mL, administered at: 15 mg/kg, Batch No.: 200-073; VetViva Richter GMBH, Wels, Austria, AMM FR/V/4109421 5/2012). Isoflurane (strength: 100 %, administered at: 0–5 %, in 100 % $O_2$ via inhalation, Batch No.: J124010; Zoetis France, Châtillon, France, AMM FR/V/9452523 4/2011) was utilized to maintain general anesthesia, as needed.

Prior to defect creation, bilateral extractions of mandibular premolars were performed (Fig. 1**a**). In brief, a full-thickness mucoperiosteal flap was followed by sectioning of the teeth in the buccal-lingual direction and extraction was carried out using root elevators and forceps without damage to the alveolar bone wall. Following teeth extraction, the buccal walls of the 3rd premolar sockets were removed through rotary instrumentation from its cervical aspect to the apical length of the socket. Four-walled semi-saddled defects (width × height = 10 mm × 10 mm) were created with depth up to the lingual wall (Fig. 1**b**). The defects were filled with porcine xenograft (Xe) putty (Batch No.: PMBURD103017; Osteogenics Biomedical, Inc., Lubbock, TX, USA) (Fig. 1**c**) and covered with either the rCOL (Fig. 1**d**) or the rPTFE (Fig. 1**e**) mem-

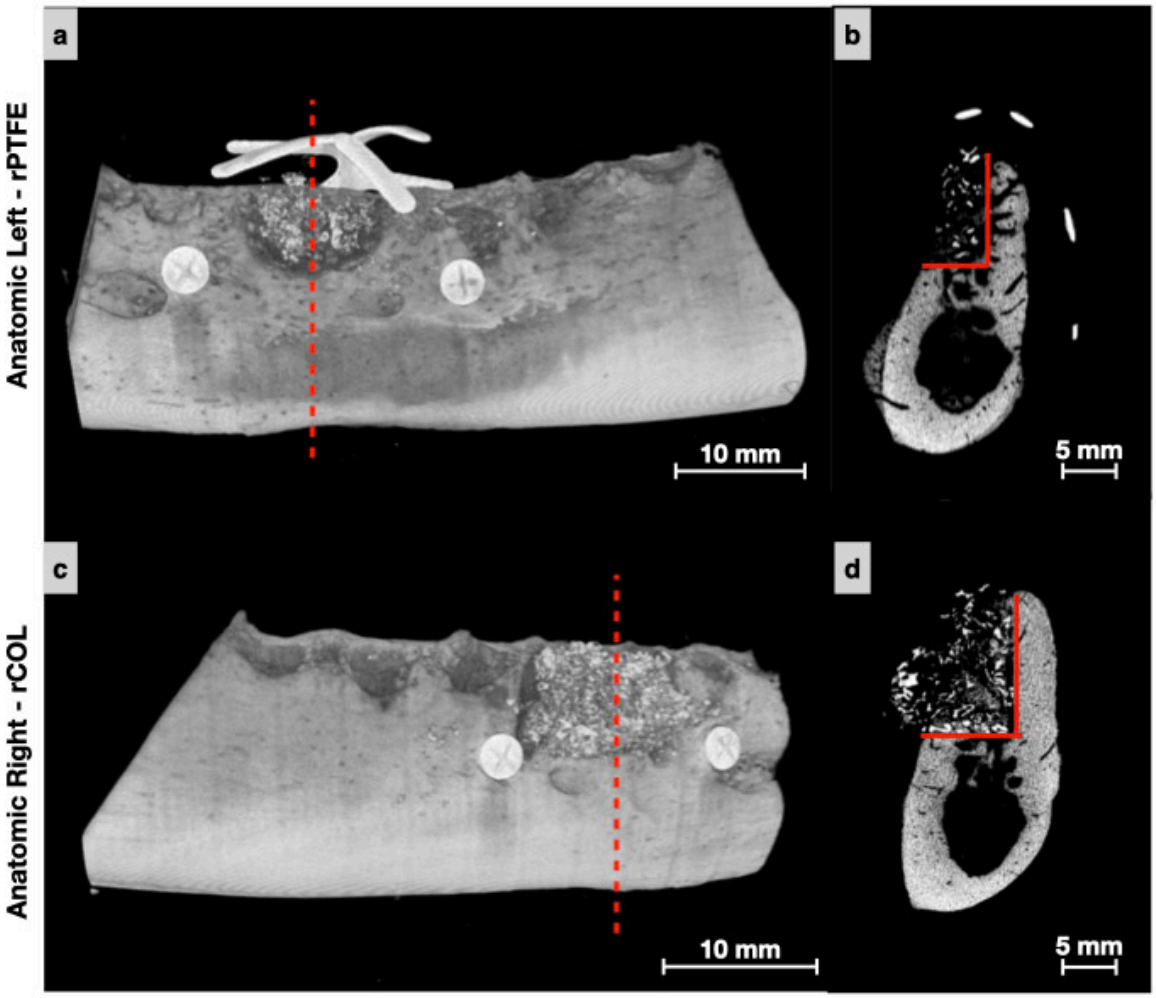


**Fig. 2. $\mu$CT overview of the mandibles.** Mandibles treated with the (**a,b**) non-resorbable (rPTFE) and (**c,d**) resorbable (rCOL) membranes. Dashed red lines (in **a,c**) indicate the location of the representative mandibular cross-sectional slices (in **b,d**) with solid red lines indicating the defect margins. Scale bars in (**a**) and (**c**) are 10 mm in length. Scale bars in (**b**) and (**d**) are 5 mm in length. $\mu$CT, microcomputed tomography.

brane. All membranes were fixed in place with 1.5 mm × 3.0 mm self-drilling screws (Batch No.: W12002A; Pro-Fix™ Precision Fixation System, Osteogenics Biomedical, Inc., Lubbock, TX, USA). Primary closure was achieved with non-resorbable sutures (3–0 PTFE, Batch No.: cs0518; Cytoplast™, Osteogenics Biomedical, Inc., Lubbock, TX, USA) (Fig. 1**f**). Senior authors (NT, LW and PGC) were aware of the group distribution throughout the course of the study duration for recordkeeping and compliance purposes.

After surgery, the animals were subjected to a soft diet for 7 days. Post-surgical medication included antibiotics (penicillin, strength: 114 mg/100 mL, administered at: 0.4–1 mL/10 kg, Batch No.: BPET2163; Vetoquinol SA, Lure, France, AMM FR/V/5680265 4/1990) and analgesics (ketoprofen, strength: 100 mg/mL, administered at: 1 mL/5 kg, Batch No.: 61133-4007; Kela N.V., Hoogstraten, Belgium, AMM FR/V/2610381 1/2011) for a period of 48 hours. All animals were euthanized after 6 weeks by means of anesthesia overdose, where animals were administered isoflurane (strength: 100 %, administered at: 0–5 %, in 100 % $O_2$ via inhalation, Batch No.: J124010; Zoetis France, Châtillon, France, AMM FR/V/9452523 4/2011), propofol (strength: 10 mg/mL, administered at: 2–8 mg/kg, via intravenous (IV), Batch No.: 379001071; Zoetis France, Châtillon, France, AMM FR/V/4197390 3/2012), and potassium chloride (strength: 40 g/120 mL, administered at: 75–150 mg/kg, via IV, Batch No.: 7447-40-7; MilliporeSigma, St. Louis, MO, USA, purity ≥99 % by titration test). The study end point was selected to closely match the critical early healing period following which PTFE membrane re-

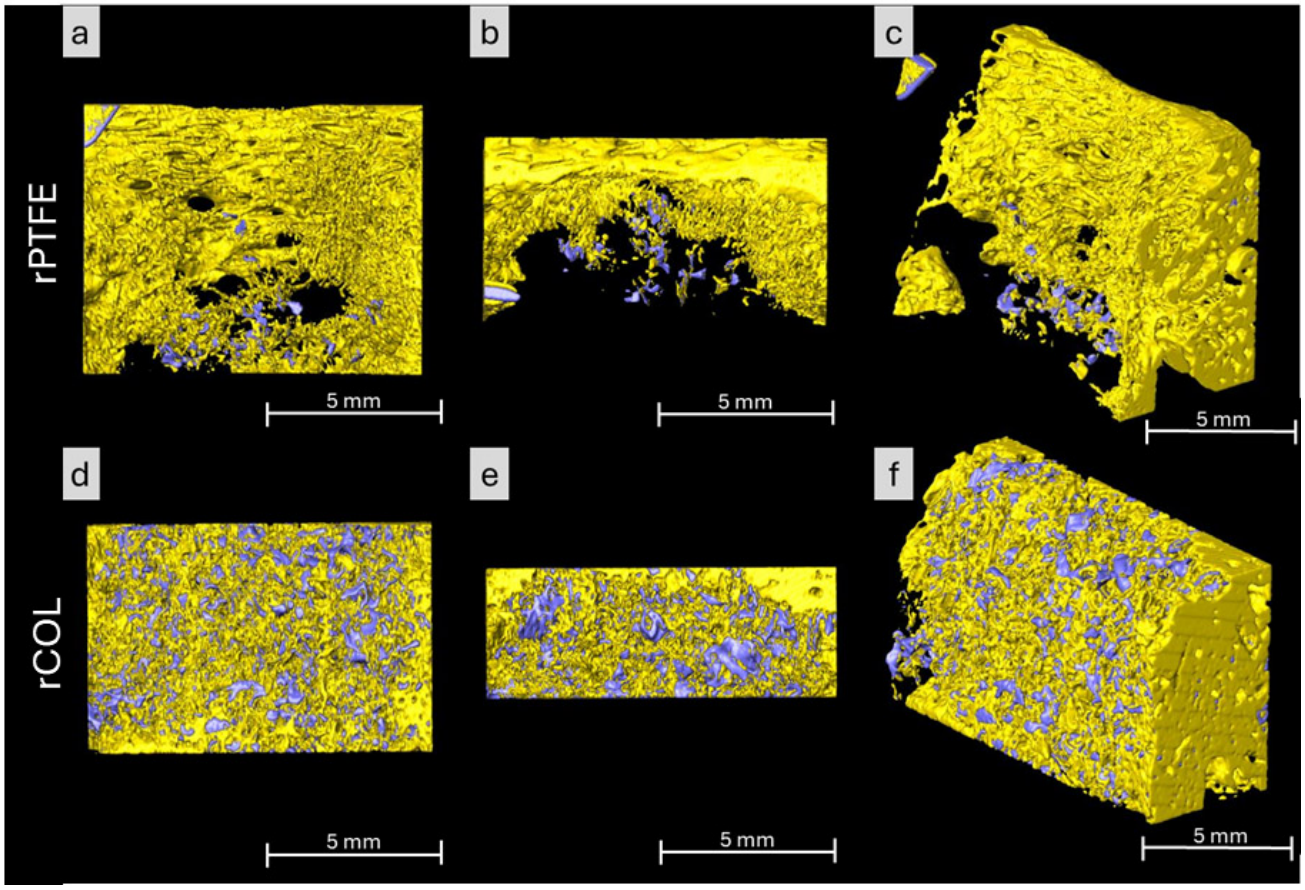


**Fig. 3. Representative 3D reconstruction of the defect sites.** (**a**) Buccal-lingual, (**b**) superior-inferior, and (**c**) isometric views of the defect volume covered with the non-resorbable (rPTFE) membrane. Representative 3D reconstructed (**d**) buccal-lingual, (**e**) superior-inferior, and (**f**) isometric views of the defect volume covered with the resorbable (rCOL) membrane. Newly formed bone is depicted in yellow and particulate graft in purple. Scale bars are 5 mm in length. 3D, three-dimensional.

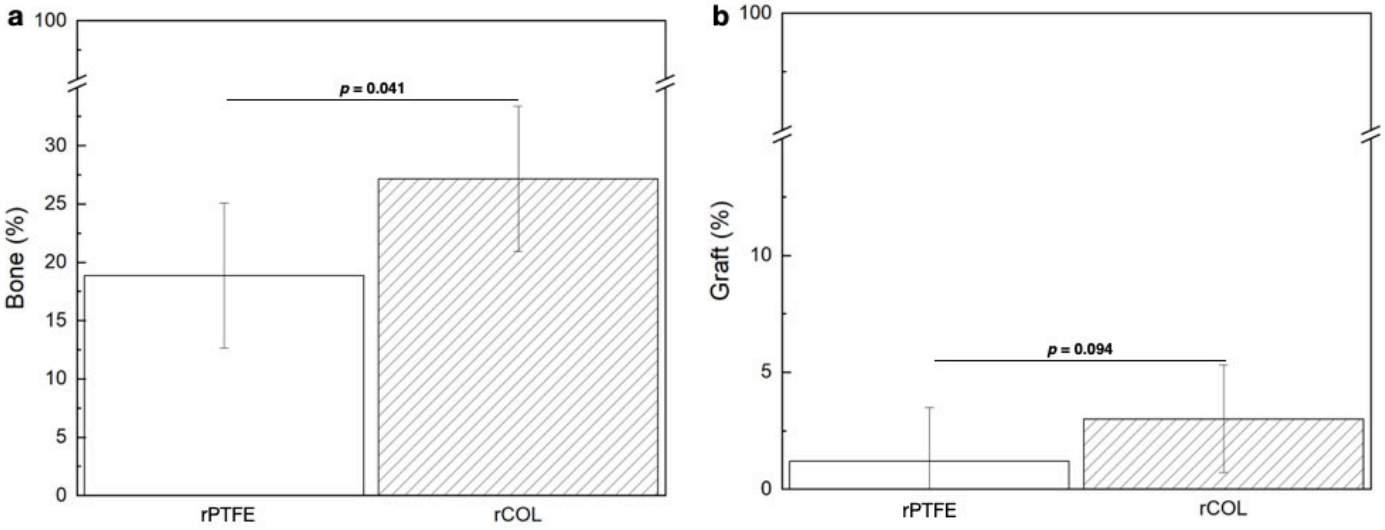


**Fig. 4. Volumetric quantification**. (**a**) Bone (%) and (**b**) Graft (%) within the defect sites, presented as means and corresponding confidence intervals, $p < 0.05$ is statistically significant.

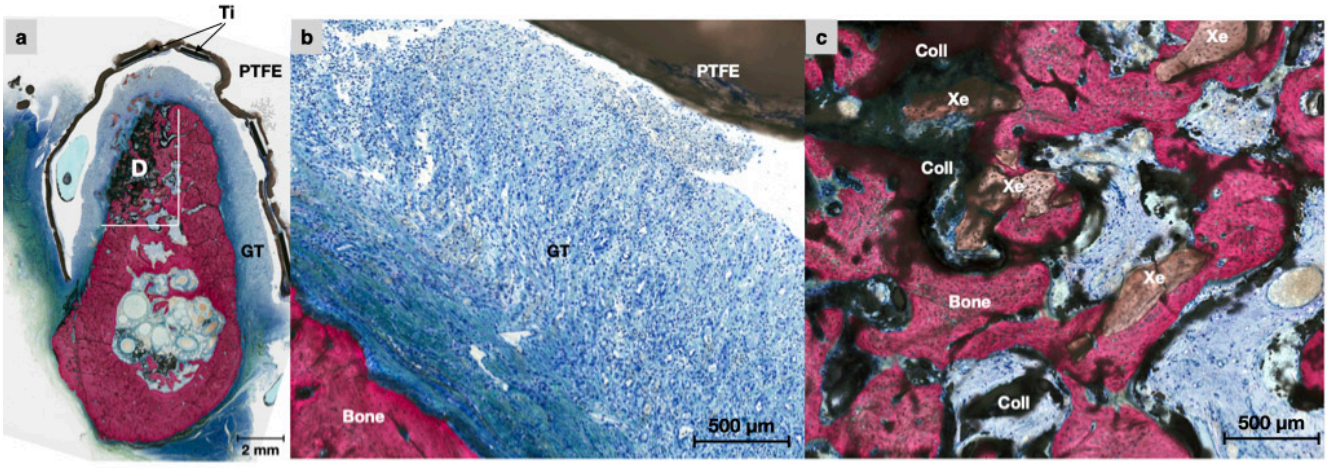


**Fig. 5. Representative histological overview of a defect treated with an rPTFE membrane.** (**a**) Survey of a representative defect (D, bounded by white lines) covered by the rPTFE membrane depicting bone (red stained) formation within the defect in a ridge that was covered by a layer of granulation tissue (GT) underneath the rPTFE membrane. Scale bar is 2 mm in length. (**b**) Higher magnification of the tissue formed between the rPTFE membrane and bone revealed granulation tissue with extensive inflammatory infiltrate and newly formed capillaries. Scale bar is 500 $\mu$m in length. (**c**) Evaluation of the grafted area showing new bone formation within the defect, where the space initially occupied by the xenograft putty material presented with a combination of newly formed bone surrounding the xenograft particles (Xe, brown stained) and within the collagen component (Coll, dark stained) of the putty. Scale bar is 500 $\mu$m in length. Ti, titanium.

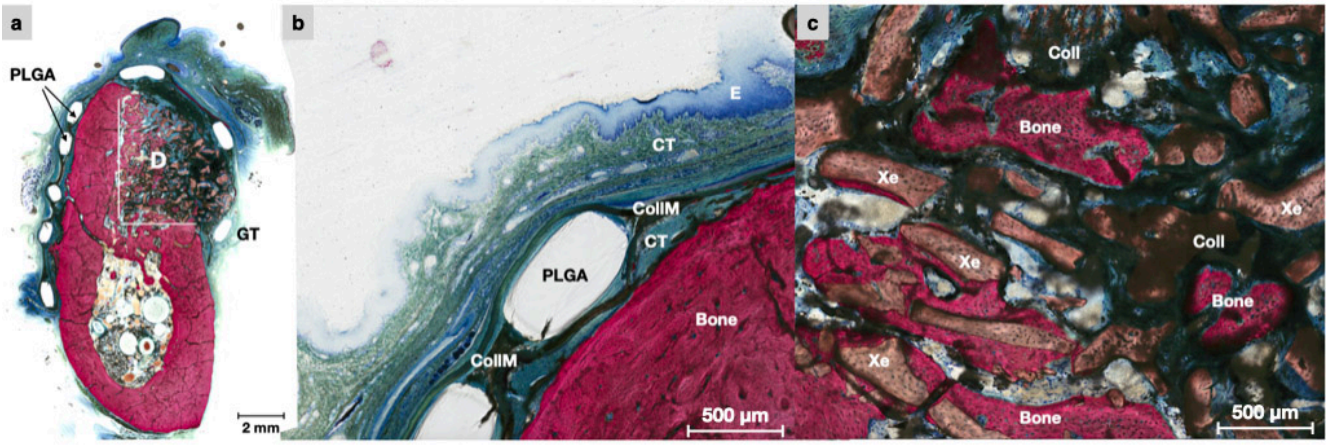


**Fig. 6. Representative histological overview of a defect treated with an rCOL membrane.** (**a**) Survey of a representative defect (D, bounded by white lines) intimately covered by the rCOL membrane (the PLGA reinforcements were continuously connected by the double collagenous layers (CollM)). Scale bar is 2 mm in length. (**b**) Higher magnification inspection of the tissue formed in proximity with the rCOL membrane revealed direct contact of the newly formed layer of connective tissue (CT)/epithelium (E), and bone at the external and internal aspects, respectively. Scale bar is 500 $\mu$m in length. (**c**) Evaluation of the grafted area showed new bone formation within the defect, where the space initially occupied by the xenograft putty material presented with a combination of newly formed bone surrounding the xenograft particles (Xe, brown stained) and collagen component (Coll, dark stained) of the putty. Scale bar is 500 $\mu$m in length. PLGA, poly-lactic-co-glycolic acid.

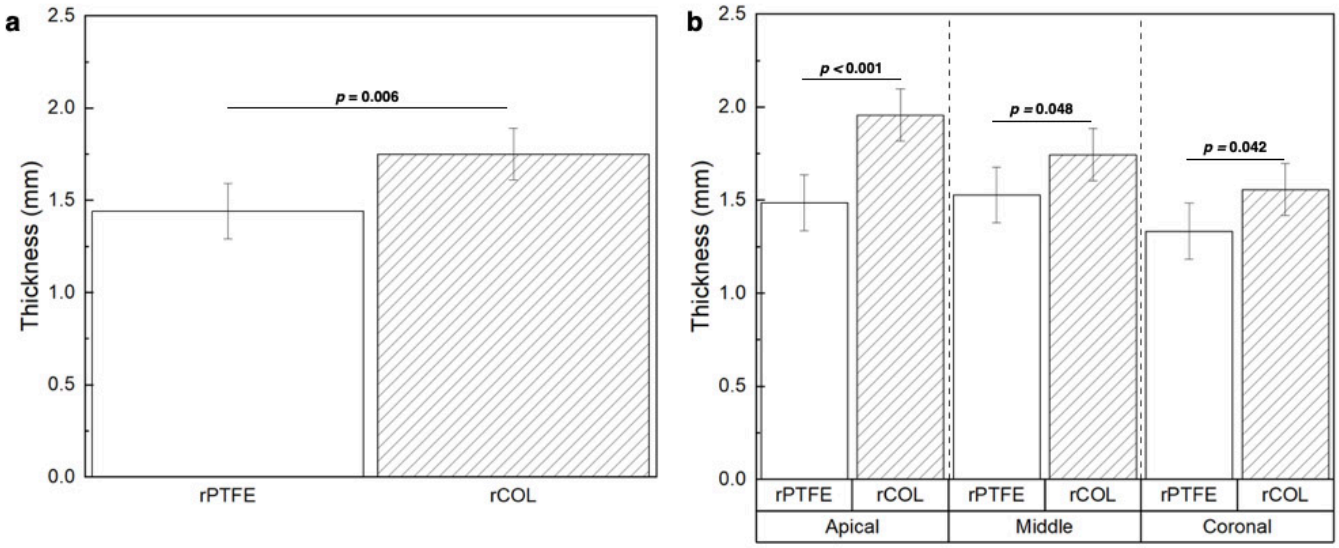


**Fig. 7. Lingual wall thickness measurements.** Measurements (**a**) collapsed over area, and (**b**) at the apical, middle, and coronal aspects. Data presented as means and corresponding confidence intervals, $p < 0.05$ is statistically significant.

moval has been recommended [17,18]. Following euthanasia, mandibles were harvested *en bloc* and immediately immersed in 10 % formalin prior to bench-top processing and analysis. No pre-established criteria for inclusion/exclusion of samples in the analysis of outcome variables were set.

### *Microcomputed Tomography and Volumetric Reconstruction*

All specimens were transferred into a 70 % ethanol solution during the microcomputed tomographic ($\mu$CT) scanning phase. Scanning was performed with a voxel resolution of 18 $\mu$m per slice, an X-ray energy level of 70 kVp, and a current level of 114 $\mu$A (Batch No.: SC4263; $\mu$CT 40, Scanco Medical, Basserdorf, Switzerland). The scan files of the mandible and defects (rPTFE: Fig. 2**a,b**; and rCOL: Fig. 2**c,d**) were imported to a three-dimensional (3D) reconstruction software (Amira 6.3.2, ThermoFisher Scientific, Waltham, MA, USA) in Digital Images and Communication in Medicine (DICOM) format to perform volumetric reconstruction and quantification. First, a virtual slice, as indicated by the dashed red lines (Fig. 2**a,c**), was acquired to assess the defect area through sagittal transections (Fig. 2**b,d**). Exposure and contrast were then adjusted to eliminate any noise or artifact and identify new bone formation. The region of interest for 3D analysis was standardized for each defect, by assessing the borders of the defect margins, indicated by solid red lines (Fig. 2**b,d**). Subsequently, the inbuilt "volume edit" tool was used to isolate the region of interest (ROI) for image segmentation. Image segmentation and digital reconstruction was performed using the Hounsfield units to select bone (16-bit grayscale threshold: 2846–5812), graft (16-bit grayscale threshold: 5812–32767), and total (16-bit grayscale threshold: 1–32767) volume of the defect. This permitted the visualization of the defect site and computation of the bone (%) and graft (%) (using the inbuilt "material statistics" tool). It is important to note that the grayscale threshold values described above are not universal and may vary as a result of changes in $\mu$CT scan settings. The $\mu$CT reconstruction and quantification was performed by a single, trained, and blinded investigator.

### *Histological Processing and Histomorphometric Analysis*

After $\mu$CT scanning, the specimens were stored in 70 % ethanol for 24 hours, and underwent progressive dehydration through a series of ethanol solutions: 70 % (24 hours), 90 % (24 hours), and 100 % (48 hours), followed by immersion in a clearing solution (methyl salicylate) for 48 hours. Samples were then infiltrated and embedded in a methacrylate-based resin followed by UV-crosslinking (for 72 hours). The resin blocks were serially-sectioned across the buccal-lingual direction of the mandible with a precision diamond saw (Batch No.: 637-IPS-02937; Isomet 1000, Buehler, Lake Bluff, IL, USA) to visualize the mandibular cross-section. Slices (~ 300 $\mu$m thick) were glued to acrylic plates using a low-viscosity, cyanoacrylate-based adhesive (Batch No.: L33BAB7000; Henkel Loctite 408, Henkel AG & Co. KGaA, Dusseldorf, Germany). After setting for 24 hours, the samples were prepared for histological/metric analysis by grinding using silicon carbide (SiC) abrasive papers (400, 600, 800, and 1200 grit) followed by polishing with a alumina-based polishing suspension (Batch No.: 5x6_SUS-R1; MicroPolish$^{TM}$ Alumina (1 $\mu$m), Buehler, Lake Bluff, IL, USA) on a grinding/polishing machine (Batch No.: 643-M3TV-10107; Metaserv 3000, Buehler, Lake Bluff, IL, USA) under copious water irrigation until a slice final thickness of ~ 90 ± 10 $\mu$m was achieved. After the final polishing steps were complete, the

slides were stained with Stevenel's Blue and Van Giesons's Picro Fuchsin (SVG) and scanned via an automated slide scanning system (Batch No.: 50178; Aperio CS2, Leica, Wetzlar, Germany). The histomorphometric analysis was made based on the measurement of three sections per defect to quantify the lingual wall thickness (mm) (Batch No.: 12.4.6; Leica Application Suite, Leica, Wetzlar, Germany). Briefly, lingual wall thickness was measured at the apical (at the inferior aspect of the lingual wall), middle (midway between the inferior and superior aspects of the lingual wall), and coronal (at the superior aspect of the lingual wall) regions by a single, trained, and blinded investigator.

*Statistical Analysis*

Statistical analysis of outcome variables (histomorphometric and volumetric data) was performed through mixed models to account for fixed and random effects. The volumetric data (Bone %) was set as the primary outcome variable. All analyses were performed using IBM SPSS (v29, IBM Corp., Armonk, NY, USA). Data was plotted as mean values with corresponding 95 % confidence interval values (mean ± 95 % CI), with $p < 0.05$ indicating significance.

## Results

*Volumetric Reconstruction and Quantification*

No animals were excluded from the analysis of outcome variables. The three-dimensional volumetric reconstruction demonstrated gradual bone ingrowth and bone bridging in the defects for both membrane groups (Fig. 3). However, quantitative volumetric analysis revealed greater bone formation (bone (%)) in the rCOL group (27.15 ± 6.22 %) relative to the rPTFE group (17.84 ± 6.22 %) ($p = 0.041$, Fig. 4**a**). Graft presence within the defect sites (graft (%)) was statistically similar ($p = 0.094$, Fig. 4**b**) between the rCOL (3.01 ± 2.31 %) and PTFE groups (1.19 ± 2.31 %) after 6 weeks of healing.

*Histological Evaluation*

Non-decalcified histological sections of the rPTFE membrane (Fig. 5**a**) revealed bone formation within the defect and a layer of granulation tissue (GT) directly underneath the membrane surface covering the defect (Fig. 5**b**). The GT formed between the rPTFE membrane and bone consisted of extensive inflammatory infiltrate and newly formed capillaries (Fig. 5**b**). In the grafted area, minimal new bone formation was observed surrounding the xenograft (Xe) putty material and within the collagen component (Coll) of the putty (Fig. 5**c**). Of note, defects treated with rPTFE presented with horizontally compromised (knife-edged) ridges at the 6-week time point accompanied by reduction in lingual wall height and thickness.

The qualitative histological observations for rCOL membrane (Fig. 6**a**) demonstrated bone formation within the defect in a ridge that was intimately covered by the rCOL membrane. The PLGA reinforcement layer was continuously connected by the double collagenous layers (CollM) (Fig. 6**b**). The tissue formed in proximity with the rCOL membrane demonstrated direct contact with a newly formed layer of connective tissue (CT)/epithelium (E), and bone at the external and internal aspects, respectively (Fig. 6**b**). Within the grafted area, the bone formation resulted in a space initially occupied by the xenograft (Xe) putty material with a combination of new bone surrounding the particles and collagen component (Coll) of the putty (Fig. 6**c**).

*Histomorphometric Evaluation*

The quantitative histomorphometric analysis was used to assess lingual wall thickness (in mm). Lingual wall thickness of defects covered with the rCOL membrane was higher relative to rPTFE (collapsed over area: 1.75 ± 0.14 mm versus 1.44 ± 0.15 mm, respectively) ($p = 0.006$, Fig. 7**a**). Similarly, rCOL demonstrated significantly higher lingual wall thickness versus rPTFE at the apical (1.95 ± 0.14 mm versus 1.48 ± 0.15 mm, respectively), middle (1.74 ± 0.14 mm versus 1.52 ± 0.15 mm, respectively), and coronal areas (1.55 ± 0.14 mm versus 1.33 ± 0.15 mm, respectively) ($p < 0.048$, Fig. 7**b**).

## Discussion

Successful rehabilitation of edentulous, atrophic defects in the oral cavity is highly dependent on the effectiveness of GBR procedures and, in turn, the barrier membrane utilized [19]. The establishment of a favorable defect environment is achieved through adequate isolation of the defect site from epithelial and connective tissue invagination [20,21]. A predictable outcome and reconstruction of bone defects within the maxillofacial region remains a concern for both surgeons and biomaterial engineers/scientists, particularly in areas where there is a need for alveolar height and thickness. Adequate alveolar ridge contour favors dental implant placement in a prosthetically-driven and biomechanically-favorable position. Biomedical research has thus focused on several novel approaches in order to improve GBR, such as different membranes to isolate the bony defects. Successful isolation is, therefore, highly dependent on the properties of barrier membranes, including structural integrity and biocompatibility [22,23]. Collagen membranes continue to garner attention as a popular option in GBR due to their favorable biological properties [24,25].

Wound healing with collagen membranes, both piscine- and mammalian- derived, has shown promising results of soft tissue healing and osteogenesis [26]. However, a major drawback and concern of collagen membranes is rapid degradation caused by collagenases breaking down the peptide bonds, thereby disrupting the structural integrity of the triple-helix and overall membrane mechanical stability [27,28]. Therefore, the purpose of this study was to further elucidate the effect of reinforcing resorbable colla-

gen membranes by comparing them to non-resorbable reinforced PTFE counterparts. PTFE membranes have been used for GBR; however, the most common complication associated with their use has been demonstrated to be wound dehiscence [6]. Furthermore, while titanium-reinforced PTFE (rPTFE) has been shown to significantly augment vertical bone regeneration, a previously conducted systematic review reported a complication rate of 4 % and 8 % with the use of d-and e-PTFE membranes, respectively [29–31]. This necessitates removal of exposed PTFE membranes following the critical early healing period where vigilant monitoring of the defect area is essential for long-term success [30]. Furthermore, it has been suggested that exposed PTFE membranes be removed 4 to 6 weeks post-surgery to reduce the risk of local infection [30]. Additionally, a secondary surgery is necessitated with the use of rPTFE membranes which could increase pain, treatment costs, and the probability of complications [31]. Contrarily, a resorbable material such as rCOL would not typically necessitate a second surgery for removal, potentially lowering aforementioned risks.

The rCOL membrane showed significantly greater lingual wall thickness relative to defects treated with rPTFE. Although both membranes resulted in gradual bone ingrowth and bone graft bridging on $\mu$CT, qualitative histology revealed that the bone formation within the defects was significantly greater within the rCOL membrane group. From a clinical perspective, successful rehabilitation of esthetic zone relies on the quality and thickness of the surrounding bone. Current evidence supports a minimum bone thickness of 2 mm around implants to achieve positive healing outcomes [32,33]. The observed 21.52 % increase in mean wall thickness with rCOL (1.75 mm versus 1.44 mm, Fig. 7**b**) approaches this recommended 2 mm threshold, which could minimize implant thread exposure in sites with thin ridges, suggesting prosthetic relevance. It can be hypothesized that the enhanced osteogenesis in the rCOL group is correlated to the prolonged barrier function of the rCOL membrane (owing to the reinforcement), which prevented the infiltration of connective tissue and epithelial tissue into the defect area. However, further investigation as to whether the reinforcement of the rCOL membrane enhanced the collagen's structural stability with regards to collagenase activity is warranted. On the other hand, as volume instability and rapid degradation kinetics are two of the primary challenges associated with the implementation of collagen membranes [34,35], strategies other than mechanical reinforcement have been explored. One such strategy is exogenous collagen crosslinking, which is the formation of covalent bonds between collagen molecules, via chemical, physical, or biological processes [36]. For example, crosslinked collagen membranes like BioMend® and Ossix Plus® exhibit extended resorption *in vivo*, but are limited by their increased fragility and brittle handling characteristics [18,37]. rCOL's PLGA mesh potentially improves drapeability while maintaining degradation control, though head-to-head studies are needed.

The granulation tissue and inflammatory infiltrate visualized on histology within the rPTFE group demonstrated complications previously seen with PTFE membranes owing to the open microstructure portion [31]. For example, macrophages respond rapidly to biomaterial implantation and are the dominant infiltrating cells [38,39]. As such, macrophages have been shown to respond and naturally bind biomaterials, once implanted [38]. As per literature, sub-micron pore sizes allow for gas exchange and permeation of small molecules, but act as a barrier towards eukaryotic cells and bacteria [40]. However, the dense lymphocyte infiltrate beneath rPTFE (Fig. 5**b**) aligns with characteristics of stage II foreign body reaction, where large pore sizes could have permitted macrophage adhesion and subsequent fusion into giant foreign-body cells [38,39]. Conversely, rCOL's submicron collagen fibril spacing may have physically restricted fusion, although this needs to be quantitatively verified in future studies.

The goal of GBR, however, is not only to promote new bone growth within the defect, but also to restore the anatomical contour of the alveolus. In this regard, the effect of the rPTFE membrane on GBR was mitigated in that the contour was qualitatively more knife-edged, with signs of horizontal compromise of the alveolus and reduced lingual wall thickness. While the current study does not provide conclusive proof of the underlying cause of this outcome, it is possible that the conventional full-thickness flap design could have resulted in insufficient healing and membrane exposure [41]. The added susceptibility of non-resorbable membranes could have resulted in tissue inflammation corroborated on the histomicrographs, leading to reduced hard tissue formation within the defect. On the contrary, collagen membranes have previously been shown to exhibit low exposure rates compared to non-resorbable counterparts, effectively reducing the occurrence of open microenvironments for bacterial infection [9]. Furthermore, collagen-based membranes have demonstrated that they accelerate early wound stabilization and initial closure of the defect in clinical settings [42,43]. While the current study did not evaluate membrane resorption or bacterial adhesion/resistance, the qualitative and quantitative evidence suggests that the rCOL membrane exhibited superior performance relative to rPTFE counterparts, warranting future studies that evaluate these *in vivo* parameters in detail.

Furthermore, hydrolysis of PLGA leads to the release of acidic monomers, resulting in a localized decrease in pH [15,44]. This acidification may cause tissue irritation and inflammation, whereby inflammatory cytokines can enhance osteoclastogenesis and prevent osteoblast activity/bone formation [44]. On the other hand, the ratio of monomers significantly affects the physicochemical properties of PLGA and is a key factor in determining its efficacy for use in biomedical applications [45]. Typically,

increasing the glycolic acid content in PLGA produces a more acidic microenvironment and accelerates degradation rates, owing to the greater hydrophilicity of glycolic acid compared to lactic acid [45]. Therefore, it is recommended that future research measures local pH levels and examines correlation with bone density gradients and bone repair observed in $\mu$CT reconstructions (e.g., Fig. 3**f**). Finally, it is imperative to recognize the limitations of this study. The current study evaluated bone regeneration solely at the 6-week time point. The encouraging outcomes observed with rCOL at this phase of the healing cascade indicate that subsequent research should investigate extended timeframes to yield an objective assessment of bone regeneration, membrane degradation, and bacterial adherence/resistance prior to clinical translation.

## Conclusions

The resorbable rCOL membranes demonstrated superior healing outcomes characterized by minimal inflammation, higher levels of bone ingrowth within the defect site, and greater lingual wall thickness compared to the non-resorbable rPTFE membranes.

## List of Abbreviations

GBR, guided bone regeneration; rCOL, reinforced collagen; PTFE, polytetrafluorethylene; rPTFE, reinforced polytetrafluorethylene; d-PTFE, high density-polytetrafluoroethylene; $\mu$CT, microcomputed tomography; PLGA, poly-lactic-co-glycolic acid; e-PTFE, expanded PTFE; ENVA, École Nationale Vétérinaire d'Alfort; 3D, three-dimensional; DICOM, Digital Images and Communication in Medicine; ROI, region of interest; SVG, Stevenel's Blue and Van Giesons's Picro Fuchsin; GT, granulation tissue; CT, connective tissue; E, epithelium; Xe, xenograft; Coll, collagen component; CollM, double collagenous layers; Ti, titanium; IV, intravenous.

## Availability of Data and Materials

All data reported in this paper will also be shared by the lead contact upon request.

## Author Contributions

NT, LW, and PGC contributed to the design of this work. EAB, KKT, ZJL, OV, SD, NT, LW, and PGC contributed to the interpretation of data and revised critically for important intellectual content. EAT and VVN analyzed the data and drafted the work. All authors read and approved the final manuscript. All authors agreed to be accountable for all aspects of the work in ensuring that questions related to the accuracy or integrity of any part of the work were appropriately investigated and resolved.

## Ethics Approval and Consent to Participate

The research protocol was approved by the Institutional Animal Care and Use Committee of École Nationale Vétérinaire d'Alfort (ENVA), Maisons-Alfort, France (approval#: 00391.01).

## Acknowledgments

We gratefully acknowledge the support of Osteogenics Biomedical, Inc., Lubbock, TX, USA.

## Funding

This work was supported by Osteogenics Biomedical, Inc., Lubbock, TX, USA.

## Conflict of Interest

The author(s) declare no conflict of interest.

## References

[1] Chappuis V, Araújo MG, Buser D. Clinical relevance of dimensional bone and soft tissue alterations post-extraction in esthetic sites. Periodontology 2000. 2017; 73: 73–83. https://doi.org/10.1111/prd.12167.

[2] Kalsi AS, Kalsi JS, Bassi S. Alveolar ridge preservation: why, when and how. British Dental Journal. 2019; 227: 264–274. https://doi.org/10.1038/s41415-019-0647-2.

[3] Mardas N, Macbeth N, Donos N, Jung RE, Zuercher AN. Is alveolar ridge preservation an overtreatment? Periodontology 2000. 2023; 93: 289–308. https://doi.org/10.1111/prd.12508.

[4] MacBeth ND, Donos N, Mardas N. Alveolar ridge preservation with guided bone regeneration or socket seal technique. A randomised, single-blind controlled clinical trial. Clinical Oral Implants Research. 2022; 33: 681–699. https://doi.org/10.1111/clr.13933.

[5] Watanabe T, Hasuike A, Wakuda S, Kogure K, Min S, Watanabe N, *et al*. Resorbable bilayer membrane made of L-lactide-ε-caprolactone in guided bone regeneration: an *in vivo* experimental study. International Journal of Implant Dentistry. 2024; 10: 1. https://doi.org/10.1186/s40729-024-00520-7.

[6] Soldatos NK, Stylianou P, Koidou VP, Angelov N, Yukna R, Romanos GE. Limitations and options using resorbable versus non-resorbable membranes for successful guided bone regeneration. Quintessence International. 2017; 48: 131–147. https://doi.org/10.3290/j.qi.a37133.

[7] Elgali I, Omar O, Dahlin C, Thomsen P. Guided bone regeneration: materials and biological mechanisms revisited. European Journal of Oral Sciences. 2017; 125: 315–337. https://doi.org/10.1111/eos.12364.

[8] Hoornaert A, d'Arros C, Heymann MF, Layrolle P. Biocompatibility, resorption and biofunctionality of a new synthetic biodegradable membrane for guided bone regeneration. Biomedical Materials. 2016; 11: 045012. https://doi.org/10.1088/1748-6041/11/4/045012.

[9] Ren Y, Fan L, Alkildani S, Liu L, Emmert S, Najman S, *et al*. Barrier Membranes for Guided Bone Regeneration (GBR): A Focus on Recent Advances in Collagen Membranes. International Journal of Molecular Sciences. 2022; 23: 14987. https://doi.org/10.3390/ijms232314987.

[10] Bartee BK, Bartee CM, inventors; Osteogenics Biomedical, Inc., assignee. Reinforced PTFE medical barriers. USA: United States patent US 8,556,990 B2. 15 October 2013.

[11] Kim YK, Ku JK. Guided bone regeneration. Journal of the Korean Association of Oral and Maxillofacial Surgeons. 2020; 46: 361–366. https://doi.org/10.5125/jkaoms.2020.46.5.361.

[12] Solomon SM, Sufaru IG, Teslaru S, Ghiciuc CM, Stafie CS. Finding the Perfect Membrane: Current Knowledge on Barrier Membranes in Regenerative Procedures: A Descriptive Review. Applied Sciences. 2022; 12: 1042. https://doi.org/10.3390/app12031042.

[13] Bergamo ETP, Balderrama ÍF, Ferreira MR, Spielman R, Slavin BV, Torroni A, *et al*. Osteogenic differentiation and reconstruction of mandible defects using a novel resorbable membrane: An *in vitro* and *in vivo* experimental study. Journal of Biomedical Materials Research. Part B, Applied Biomaterials. 2023; 111: 1966–1978. https://doi.org/10.1002/jbm.b.35299.

[14] Bartee BK, Cain E, inventors; Osteogenics Biomedical, Inc., assignee. Multi-layer collagen-based membrane. USA: United States patent US 2022/0184275 A1. 16 June 2022.

[15] Lu Y, Cheng D, Niu B, Wang X, Wu X, Wang A. Properties of Poly (Lactic-co-Glycolic Acid) and Progress of Poly (Lactic-co-Glycolic Acid)-Based Biodegradable Materials in Biomedical Research. Pharmaceuticals. 2023; 16: 454. https://doi.org/10.3390/ph16030454.

[16] Zhao D, Zhu T, Li J, Cui L, Zhang Z, Zhuang X, *et al*. Poly(lactic-*co*-glycolic acid)-based composite bone-substitute materials. Bioactive Materials. 2020; 6: 346–360. https://doi.org/10.1016/j.bioactmat.2020.08.016.

[17] Matumoto EK, Corrêa MG, Couso-Queiruga E, Monteiro MF, Graham Z, Braz SHG, *et al*. Influence of partially exposed nonabsorbable membrane for alveolar ridge preservation: A randomized controlled trial. Clinical Implant Dentistry and Related Research. 2023; 25: 447–457. https://doi.org/10.1111/cid.13202.

[18] Mizraji G, Davidzohn A, Gursoy M, Gursoy U, Shapira L, Wilensky A. Membrane barriers for guided bone regeneration: An overview of available biomaterials. Periodontology 2000. 2023; 93: 56–76. https://doi.org/10.1111/prd.12502.

[19] Wessing B, Lettner S, Zechner W. Guided Bone Regeneration with Collagen Membranes and Particulate Graft Materials: A Systematic Review and Meta-Analysis. The International Journal of Oral & Maxillofacial Implants. 2018; 33: 87–100. https://doi.org/10.11607/jomi.5461.

[20] Urban IA, Monje A. Guided Bone Regeneration in Alveolar Bone Reconstruction. Oral and Maxillofacial Surgery Clinics of North America. 2019; 31: 331–338. https://doi.org/10.1016/j.coms.2019.01.003.

[21] Sheikh Z, Qureshi J, Alshahrani AM, Nassar H, Ikeda Y, Glogauer M, *et al*. Collagen based barrier membranes for periodontal guided bone regeneration applications. Odontology/The Society of the Nippon Dental University. 2017; 105: 1–12. https://doi.org/10.1007/s10266-016-0267-0.

[22] Nayak VV, Mirsky NA, Slavin BV, Witek L, Coelho PG, Tovar N. Non-Thermal Plasma Treatment of Poly(tetrafluoroethylene) Dental Membranes and Its Effects on Cellular Adhesion. Materials. 2023; 16: 6633. https://doi.org/10.3390/ma16206633.

[23] Yang Z, Wu C, Shi H, Luo X, Sun H, Wang Q, *et al*. Advances in Barrier Membranes for Guided Bone Regeneration Techniques. Frontiers in Bioengineering and Biotechnology. 2022; 10: 921576. https://doi.org/10.3389/fbioe.2022.921576.

[24] Aprile P, Letourneur D, Simon-Yarza T. Membranes for Guided Bone Regeneration: A Road from Bench to Bedside. Advanced Healthcare Materials. 2020; 9: e2000707. https://doi.org/10.1002/adhm.202000707.

[25] Cramer MC, Badylak SF. Extracellular Matrix-Based Biomaterials and Their Influence Upon Cell Behavior. Annals of Biomedical Engineering. 2020; 48: 2132–2153. https://doi.org/10.1007/s10439-019-02408-9.

[26] Sheinberg DS, Almada R, Parra M, Slavin BV, Mirsky NA, Nayak VV, *et al*. Preclinical evaluation of mucogingival defect treatment using piscine membranes: An *in vivo* assessment of wound healing. Journal of Biomedical Materials Research. Part B, Applied Biomaterials. 2024; 112: e35468. https://doi.org/10.1002/jbm.b.35468.

[27] Shi X, Li X, Tian Y, Qu X, Zhai S, Liu Y, *et al*. Physical, mechanical, and biological properties of collagen membranes for guided bone regeneration: a comparative *in vitro* study. BMC Oral Health. 2023; 23: 510. https://doi.org/10.1186/s12903-023-03223-4.

[28] Amirrah IN, Lokanathan Y, Zulkiflee I, Wee MFMR, Motta A, Fauzi MB. A Comprehensive Review on Collagen Type I Development of Biomaterials for Tissue Engineering: From Biosynthesis to Bioscaffold. Biomedicines. 2022; 10: 2307. https://doi.org/10.3390/biomedicines10092307.

[29] Urban IA, Montero E, Monje A, Sanz-Sánchez I. Effectiveness of vertical ridge augmentation interventions: A systematic review and meta-analysis. Journal of Clinical Periodontology. 2019; 46: 319–339. https://doi.org/10.1111/jcpe.13061.

[30] Zeller AN, Schenk R, Bonsmann M, Stockbrink G, Becher S, Pabst A. Complication rates of guided bone regeneration using titanium-reinforced PTFE membranes: a retrospective analysis. Clinical Oral Investigations. 2024; 28: 616. https://doi.org/10.1007/s00784-024-06007-4.

[31] Zhang M, Zhou Z, Yun J, Liu R, Li J, Chen Y, *et al*. Effect of Different Membranes on Vertical Bone Regeneration: A Systematic Review and Network Meta-Analysis. BioMed Research International. 2022; 2022: 7742687. https://doi.org/10.1155/2022/7742687.

[32] Alssum L, Al-Kattan R, Al-Shibani N, Al Ali H, Aldossari F, Allam E. Clinical and Radiographic Evaluation of Bone Profile Around Dental Implants Placed in the Esthetic Zone. Journal of Multidisciplinary Healthcare. 2025; 18: 591–601. https://doi.org/10.2147/jmdh.S503269.

[33] Liñares A, Dopico J, Magrin G, Blanco J. Critical review on bone grafting during immediate implant placement. Periodontology 2000. 2023; 93: 309–326. https://doi.org/10.1111/prd.12516.

[34] Vallecillo C, Toledano-Osorio M, Vallecillo-Rivas M, Toledano M, Osorio R. *In Vitro* Biodegradation Pattern of Collagen Matrices for Soft Tissue Augmentation. Polymers. 2021; 13: 2633. https://doi.org/10.3390/polym13162633.

[35] Wu Y, Chen S, Luo P, Deng S, Shan Z, Fang J, *et al*. Optimizing the bio-degradability and biocompatibility of a biogenic collagen membrane through cross-linking and zinc-doped hydroxyapatite. Acta Biomaterialia. 2022; 143: 159–172. https://doi.org/10.1016/j.actbio.2022.02.004.

[36] Sorushanova A, Delgado LM, Wu Z, Shologu N, Kshirsagar A, Raghunath R, *et al*. The Collagen Suprafamily: From Biosynthesis to Advanced Biomaterial Development. Advanced Materials. 2019; 31: e1801651. https://doi.org/10.1002/adma.201801651.

[37] Radenković M, Alkildani S, Stoewe I, Bielenstein J, Sundag B, Bellmann O, *et al*. Comparative *In Vivo* Analysis of the Integration Behavior and Immune Response of Collagen-Based Dental Barrier Membranes for Guided Bone Regeneration (GBR). Membranes. 2021; 11: 712. https://doi.org/10.3390/membranes11090712.

[38] Sheikh Z, Brooks PJ, Barzilay O, Fine N, Glogauer M. Macrophages, Foreign Body Giant Cells and Their Response to Implantable Biomaterials. Materials. 2015; 8: 5671–5701. https://doi.org/10.3390/ma8095269.

[39] Zhou X, Wang Y, Ji J, Zhang P. Materials Strategies to Overcome the Foreign Body Response. Advanced Healthcare Materials. 2024; 13: e2304478. https://doi.org/10.1002/adhm.202304478.

[40] Nocca G, Filetici P, Bugli F, Mordente A, D'Addona A, Dassatti L. Permeability of P. gingivalis or its metabolic products through collagen and dPTFE membranes and their effects on the viability of osteoblast-like cells: an *in vitro* study. Odontology/The Society of the Nippon Dental University. 2022; 110: 710–718. https://doi.org/10.1007/s10266-022-00705-9.

[41] Windisch P, Orban K, Salvi GE, Sculean A, Molnar B. Vertical-guided bone regeneration with a titanium-reinforced d-PTFE membrane utilizing a novel split-thickness flap design: a prospective case series. Clinical Oral Investigations. 2021; 25: 2969–2980. https://doi.org/10.1007/s00784-020-03617-6.

[42] Kumari CBN, Ramakrishnan T, Devadoss P, Vijayalakshmi R, Alzahrani KJ, Almasri MA, *et al*. Use of Collagen Membrane in the Treatment of Periodontal Defects Distal to Mandibular Second Molars Following Surgical Removal of Impacted Mandibular Third Molars: A Comparative Clinical Study. Biology. 2021; 10: 1348. https://doi.org/10.3390/biology10121348.

[43] Gueldenpfennig T, Houshmand A, Najman S, Stojanovic S, Korzinskas T, Smeets R, *et al*. The Condensation of Collagen Leads to an Extended Standing Time and a Decreased Pro-inflammatory Tissue Response to a Newly Developed Pericardium-based Barrier Membrane for Guided Bone Regeneration. *In Vivo*. 2020; 34: 985–1000. https://doi.org/10.21873/invivo.11867.

[44] Go EJ, Kang EY, Lee SK, Park S, Kim JH, Park W, *et al*. An osteoconductive PLGA scaffold with bioactive $\beta$-TCP and anti-inflammatory $Mg(OH)_2$ to improve *in vivo* bone regeneration. Biomaterials Science. 2020; 8: 937–948. https://doi.org/10.1039/c9bm01864f.

[45] Yang J, Zeng H, Luo Y, Chen Y, Wang M, Wu C, *et al*. Recent Applications of PLGA in Drug Delivery Systems. Polymers. 2024; 16: 2606. https://doi.org/10.3390/polym16182606.

**Editor's note**: The Scientific Editor responsible for this paper was Matteo D'Este.

**Received**: 6th May 2025; **Accepted**: 8th September 2025; **Published**: 31st December 2025